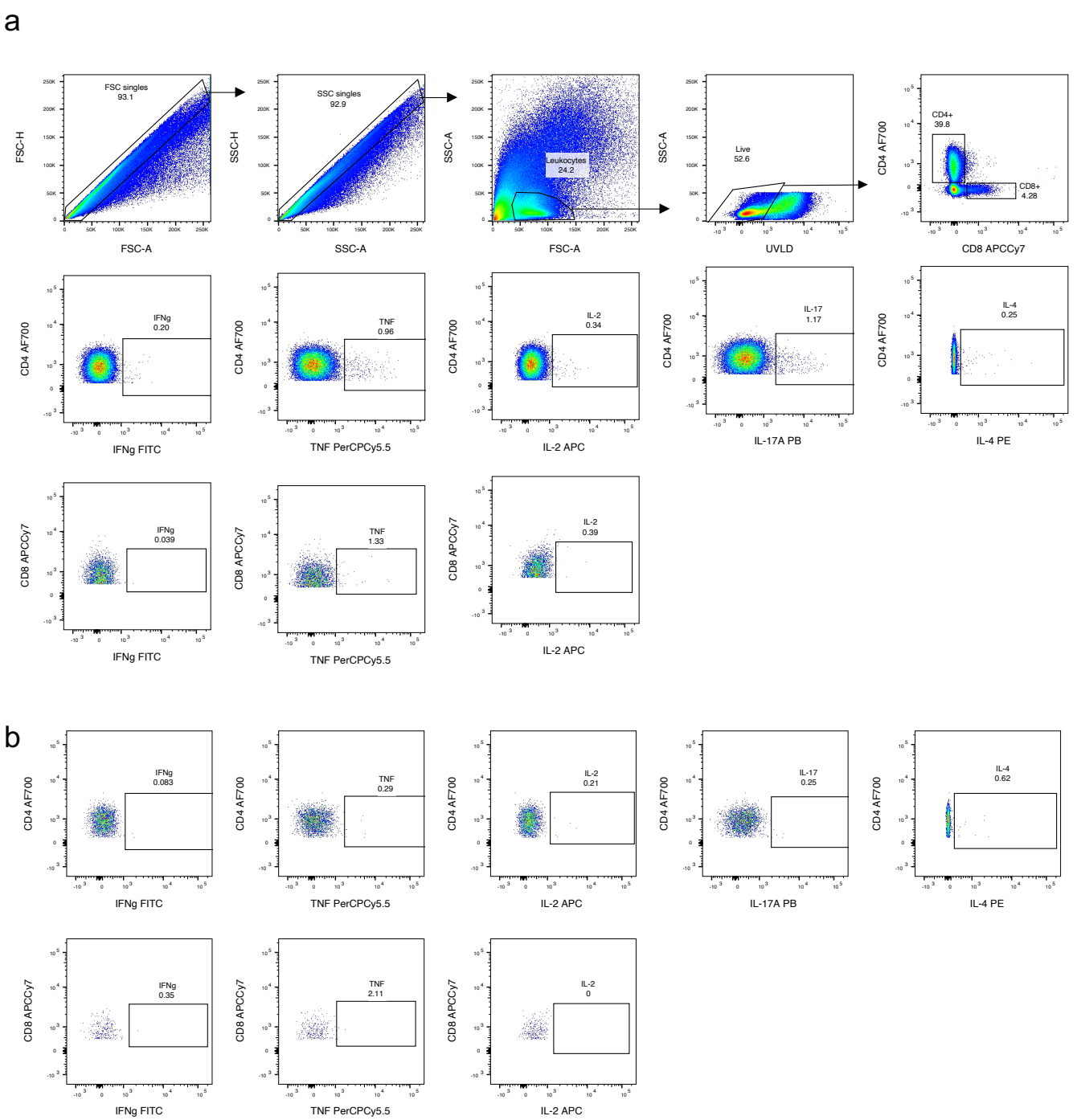

Figure S1. Gating strategy for analysis of flow cytometry data, to quantitate the proportion of Spike-specific cytokine producing T-cells in the lungs or spleen. After quality control gates to exclude doublets and debris, live cells were gated, then $CD4^+$ and $CD8^+$ cells. Cytokine positive cells for each T-cell population were gated. A representative lung sample is shown (WT mouse reconstituted with *Tlr2-/-* BM, vaccinated intra-nasally with Pam_2Cys Spike three times two weeks apart) after *ex vivo* stimulation in the presence of Brefeldin A with (**a**) Spike protein (10 µg/ml) or (**b**) no protein recall, used as a negative control to set gates for cytokine producing cells.

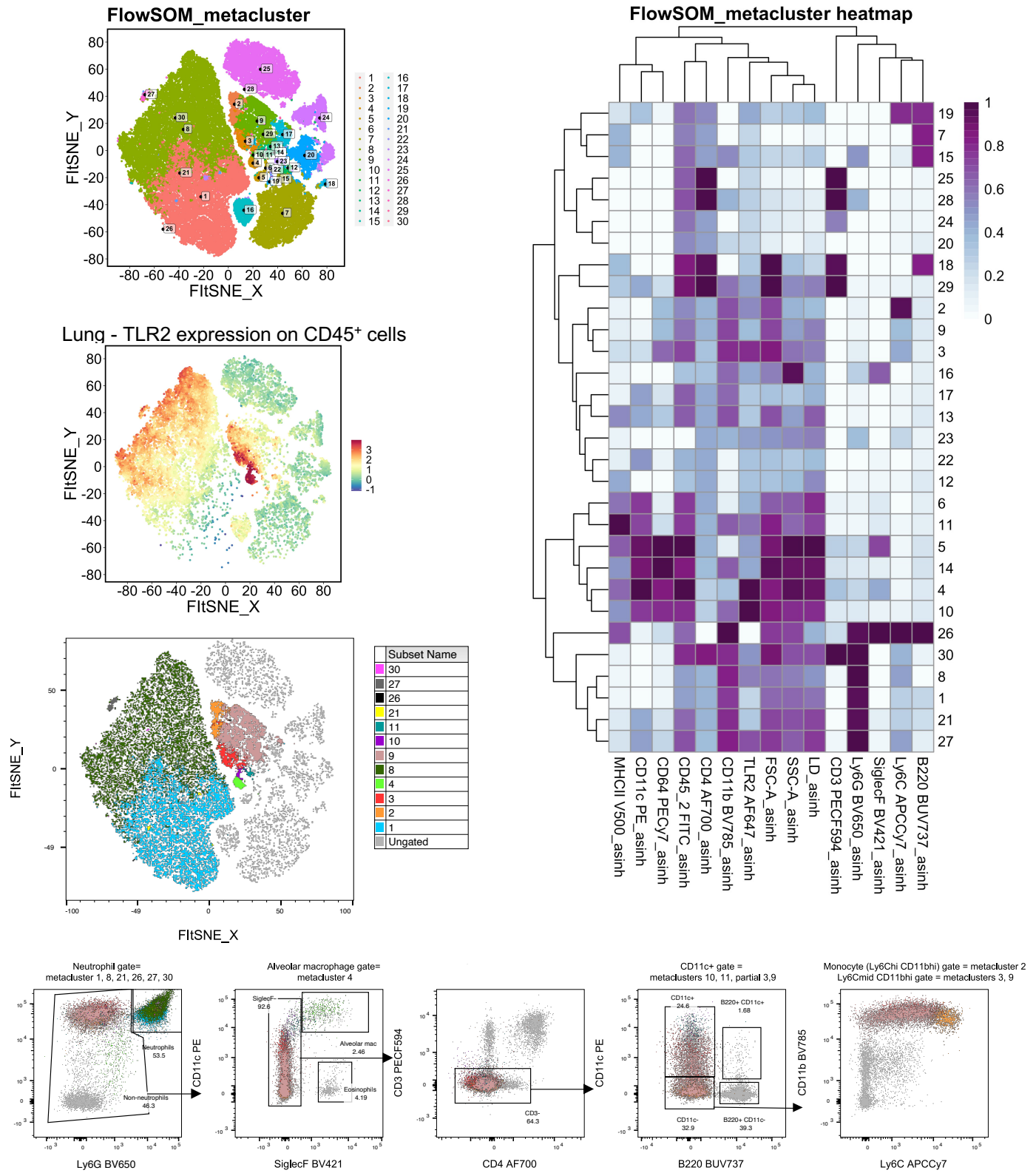

Figure S2. Computational analysis of lung immune cells 24 hours post Pam_2Cys Spike i.n. Unsupervised clustering of lung $CD45^+$ cells was performed on flow cytometry data using the Spectre R package. All 30 metaclusters are indicated, alongside their relative expression of surface phenotypic markers. Relative expression of TLR2 across the clusters was examined by FIt-SNE, a representative plot for WT (BALB/c) mice receiving WT bone marrow is shown. Clusters localizing with upregulated TLR2 expression were subjected to manual gating in FlowJo to confirm cell phenotypes. Clusters 1, 8, 21, 26, 27 and 30 were phenotypically neutrophils ($Ly6G^+CD11b^+$; these metaclusters excluded from subsequent gating). Cluster 4, which had the highest degree of TLR2 expression were alveolar macrophages ($SiglecF^+CD11c^{hi}$; excluded from subsequent gating). Metaclusters 10 and 11 which also had high TLR2 were $SiglecF^-CD11c^+$ (excluded from subsequent gating), cluster 2 were monocytes ($Ly6C^{hi}CD11b^{hi}$) and clusters 3 and 9 were $CD11c^{-\text{ to mid}}Ly6C^{mid}CD11b^{hi}$.

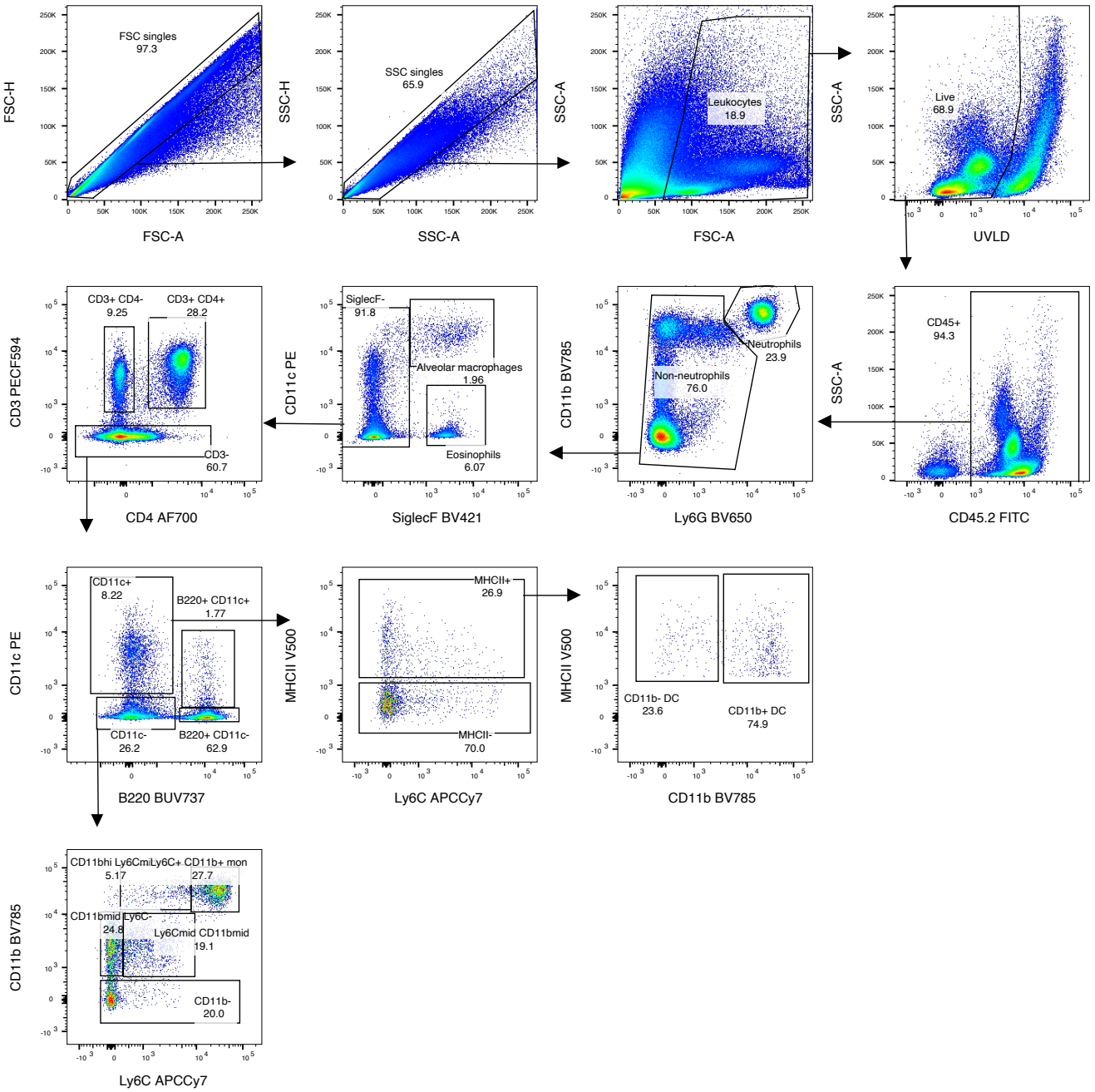

Figure S3. Gating strategy for analysis of flow cytometry data, to characterize lung and broncho-alveolar immune populations described in figures 3 and S4-6. After quality control gates to exclude doublets and debris, live cells were gated, then CD45$^+$ cells. Neutrophils (Ly6G$^+$CD11b$^+$) were gated, then alveolar macrophages (SiglecF$^+$CD11c^{hi}) and eosinophils (SiglecF^{hi}CD11c^{lo}). SiglecF$^-$ cells were gated and T-cells defined (CD4$^+$CD3$^-$, CD4$^-$CD3$^+$). CD3$^-$ cells were divided into B220$^+$CD11c$^+$, B220$^+$CD11c$^-$, B220$^-$CD11c$^+$ and B220$^-$CD11c$^-$. B220$^-$CD11c$^+$ cells were divided into MHCII$^-$ and MHCII$^+$, then MHCII$^+$ cells divided between CD11b$^+$ and CD11b$^-$. B220$^-$CD11c$^-$ cells were divided into 5 populations based on Ly6C and CD11b expression.

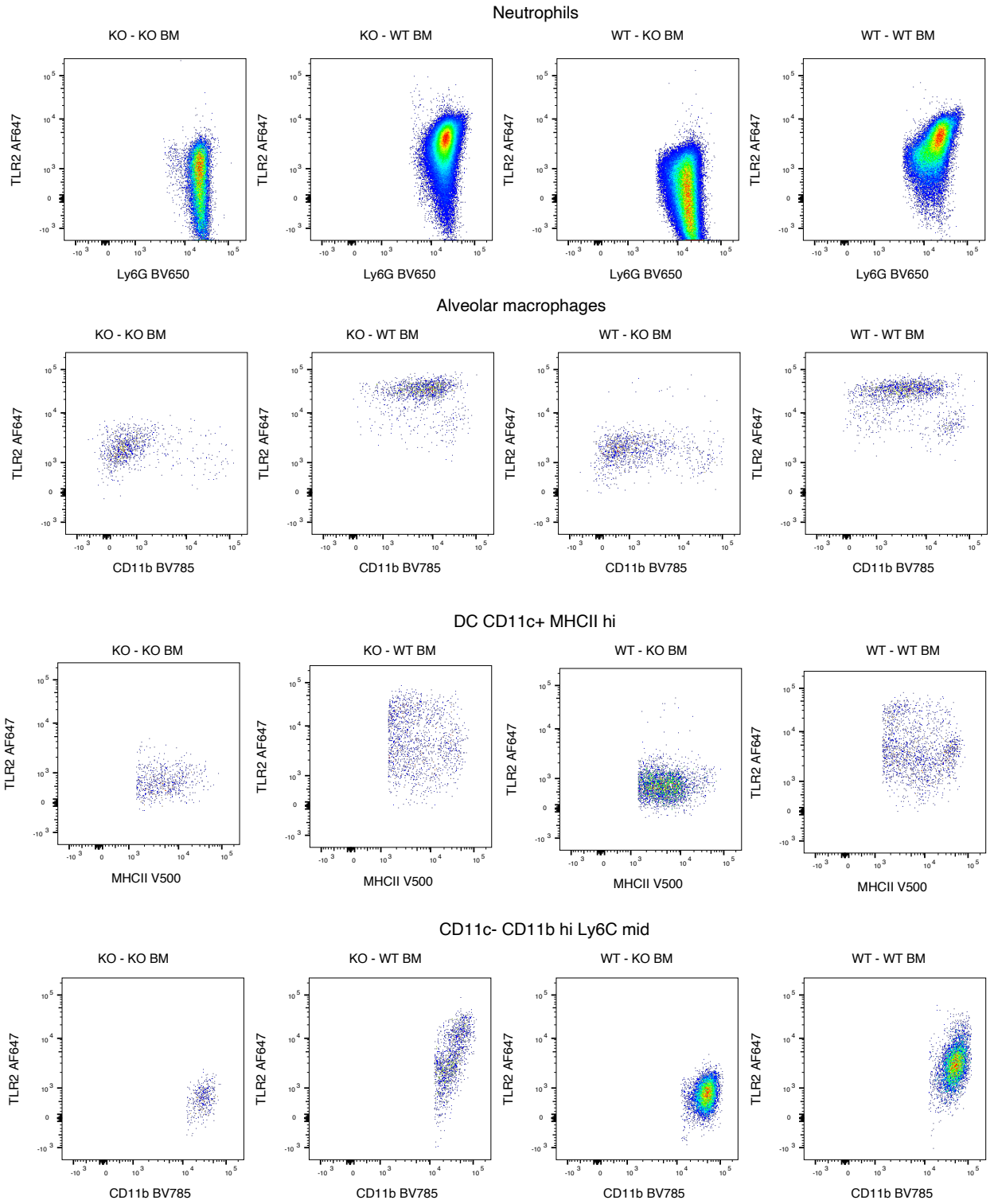

Figure S4. *Tlr2-/-* (KO) or wild type (WT) mice (n=6) were irradiated then received transfer of *Tlr2-/-* or WT bone marrow (BM) cells i.v. Mice were rested for 12 weeks to allow hematopoietic reconstitution and replacement, then were immunized with Pam_2Cys Spike intra-nasally. Immune cells in the lungs were characterized at 24 hours post vaccination by flow cytometry. Expression of TLR2 on key lung populations of interest, a representative sample from each experimental group is shown.

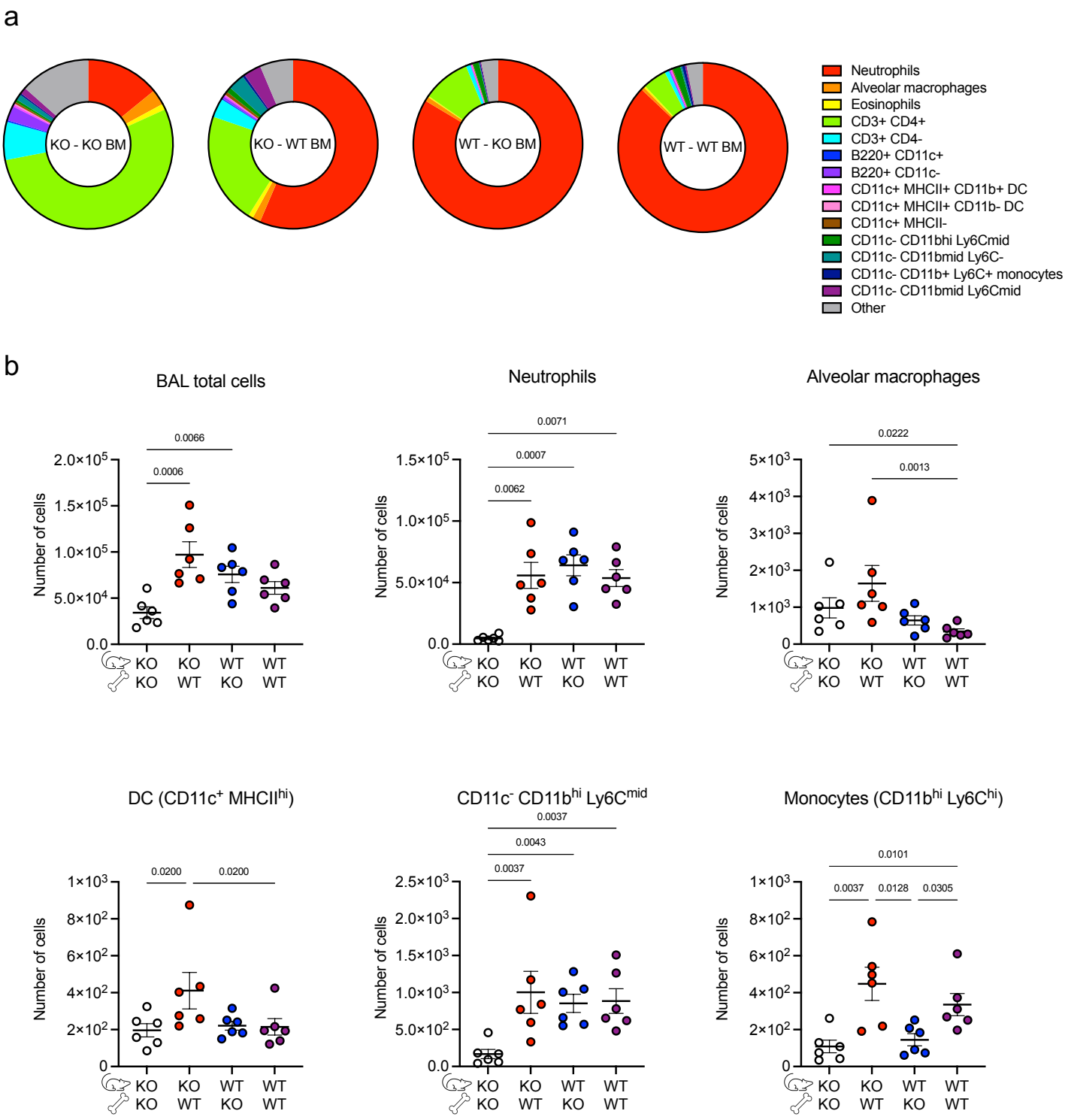

Figure S5. TLR2 expression by both hematopoietic and non-hematopoietic lineages contribute to early innate immune responses in the airways to mucosal vaccination with Pam_2Cys Spike. *Tlr2-/-* (KO) or wild type (WT) mice (n=6) were lethally irradiated then received transfer of *Tlr2-/-* or WT bone marrow (BM) cells i.v. Mice were rested for 12 weeks to allow hematopoietic reconstitution and replacement, then immunized with Pam_2Cys Spike intra-nasally. Immune cells in the airways (BALF) were characterized at 24 hours post vaccination. (**A**) Mean proportions of $CD45^+$ cell populations in the BALF determined by flow cytometry, with (**B**) quantitation of populations of interest. Data are for individual mice (n=6), means +/- SEM are shown. Statistics: Kruskal-Wallis test, Dunn's multiple comparisons, p values are indicated.

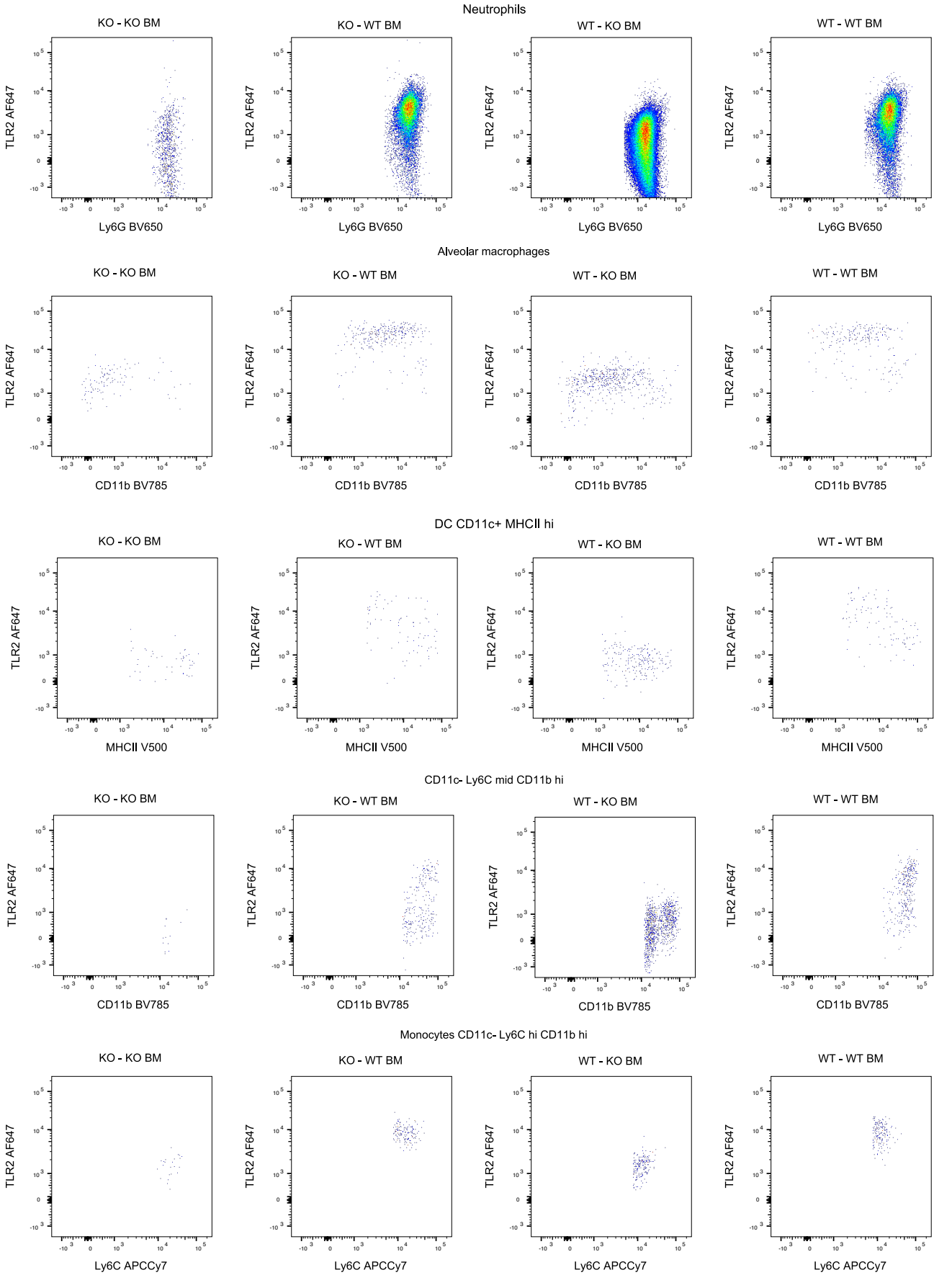

Figure S6. *Tlr2-/-* (KO) or wild type (WT) mice (n=6) were lethally irradiated then received transfer of *Tlr2-/-* or WT bone marrow (BM) cells i.v. Mice were rested for 12 weeks to allow hematopoietic reconstitution and replacement, then were immunized with Pam_2Cys Spike intra-nasally. Immune cells in the airways were characterized at 24 hours post vaccination by flow cytometry. Expression of TLR2 on key airway (BALF) populations of interest, a representative sample from each experimental group is shown.

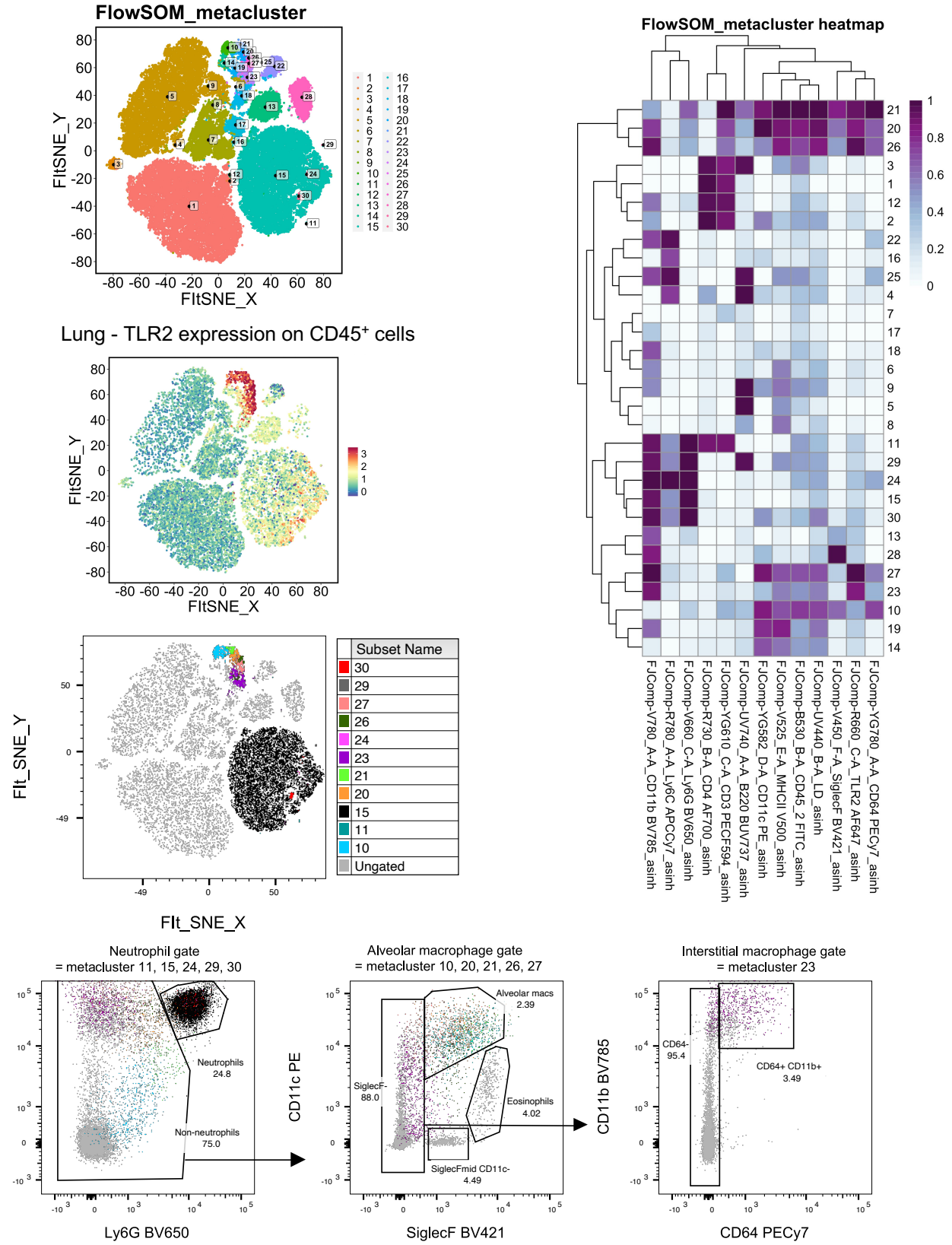

Figure S7. Computational analysis of lung immune cells one week post Pam_2Cys Spike i.n final booster vaccination. Unsupervised clustering of lung $CD45^+$ cells was performed on flow cytometry data using the Spectre R package. All 30 metaclusters are indicated, alongside their relative expression of surface phenotypic markers. Relative expression of TLR2 across the clusters was examined by FIt-SNE, a representative plot for WT (BALB/c) mice receiving WT bone marrow is shown. Clusters localizing with upregulated TLR2 expression were subjected to manual gating in FlowJo to confirm cell phenotypes. Clusters 11, 15, 24, 29 and 30, which had low to moderate TLR2 expression, were phenotypically neutrophils ($Ly6G^+CD11b^+$; these metaclusters excluded from subsequent gating). Clusters 10, 20, 21, 26 and 27, which localized with high TLR2 expression, were primarily alveolar macrophages ($SiglecF^+CD11c^{hi}$; excluded from subsequent gating) and metacluster 23 were interstitial macrophages ($SiglecF^-CD64^+CD11b^{hi}$).

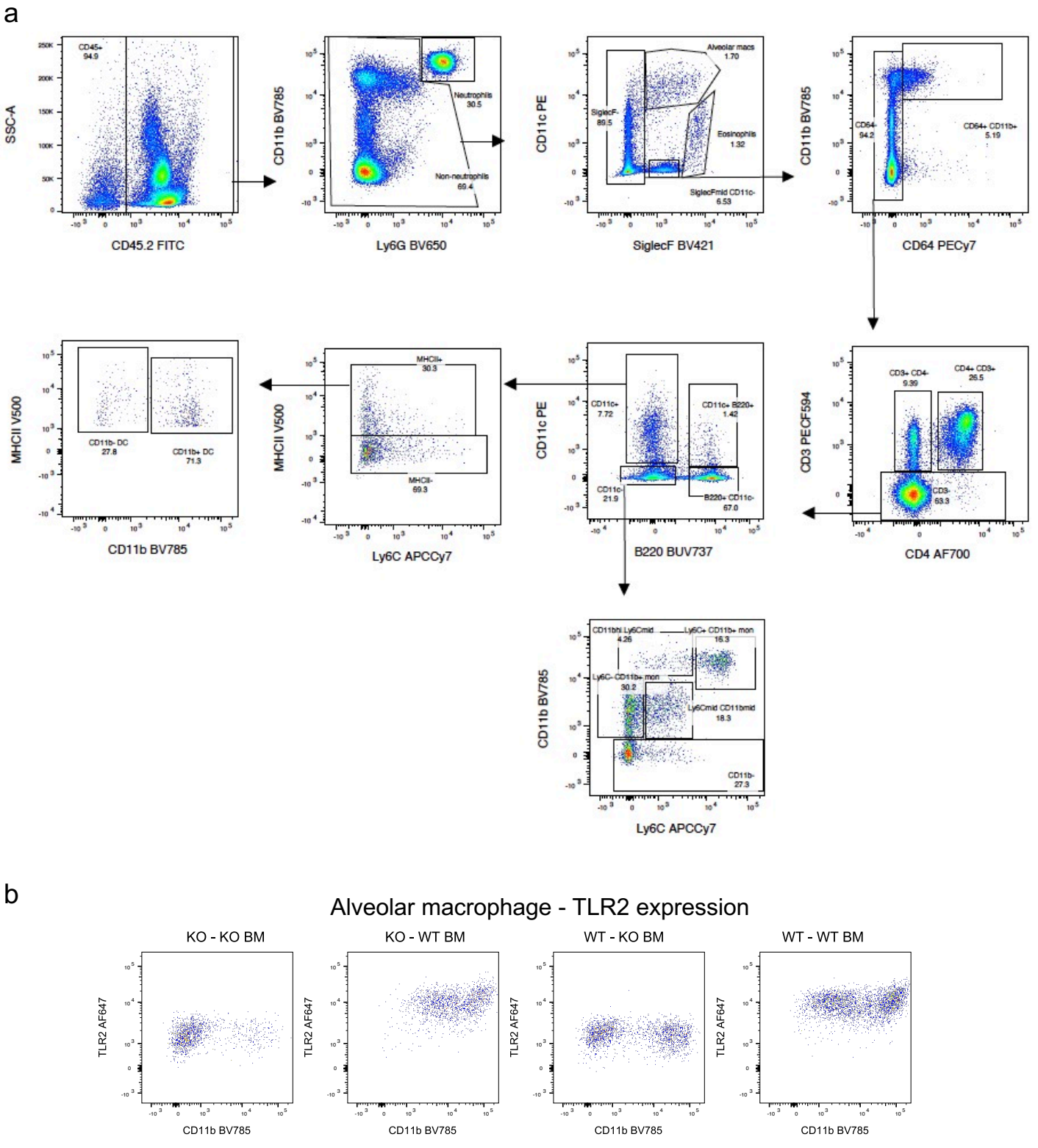

Figure S8. (**a**) Gating strategy for analysis of flow cytometry data, to characterize lung immune populations described in figure 4. After quality control gates to exclude doublets and debris, live cells were gated, then CD45$^+$ cells. Neutrophils (Ly6G$^+$CD11b$^+$) were gated, then alveolar macrophages (SiglecF$^+$CD11c^{hi}), eosinophils (SiglecF^{hi}CD11c$^{lo\text{-}int}$), and SiglecF^{int}CD11c^{lo} cells. SiglecF$^-$ cells were gated and divided into interstitial macrophages (CD64$^+$CD11b^{hi}) and CD64$^-$ cells. T-cells were defined (CD4$^+$CD3$^-$, CD4$^-$CD3$^+$), then CD3$^-$ cells divided into B220$^+$CD11c$^+$, B220$^+$CD11c$^-$, B220$^-$CD11c$^+$ and B220$^-$CD11c$^-$. B220$^-$CD11c$^+$ cells were divided into MHCII$^-$ and MHCII$^+$, then MHCII$^+$ cells divided between CD11b$^+$ and CD11b$^-$. B220$^-$CD11c$^-$ cells were divided into 5 populations based on Ly6C and CD11b expression. (**b**) Comparison of TLR2 expression on alveolar macrophages, a representative sample from each experimental group (from Figure 4) is shown.

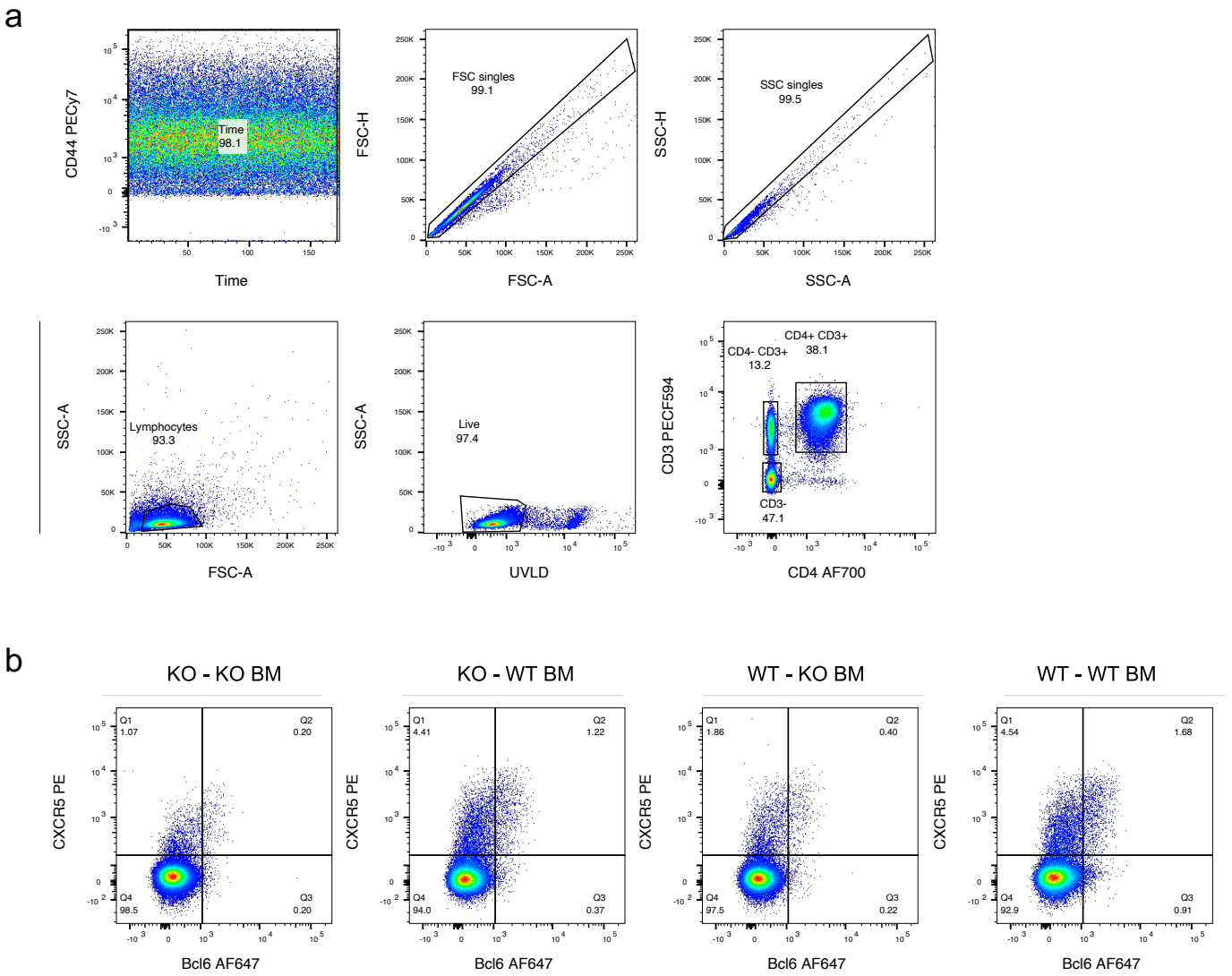

Figure S9. (**a**) Gating strategy for analysis of flow cytometry data, to quantitate the proportion of Bcl6^{+} CD4^{+} T-cells in the mediastinal lymph node of mucosally vaccinated mice. After quality control gates to exclude doublets and debris, live cells were gated, then CD4^{+}CD3^{+} cells. (**b**) Comparison of Bcl6^{+} CD4^{+} T-cells, a representative sample from each experimental group (from Figure 5) is shown.